CHARACTERIZATION OF LATERALLY CONTIGUOUS PHYLLOSILICATE DEPOSITS IN WEST MARGARITIFER TERRA, MARS. K. D. Seelos[1], R. E. Maxwell[2,1], F. P. Seelos[1], D L. Buczkowski[1], and C. E. Viviano-Beck[1], C. M. Weitz[3], [1]JHU Applied Physics Laboratory, Laurel, MD (kim.seelos@jhuapl.edu); [2]Dept. of Earth and Planetary Sciences, UCSC, Santa Cruz, CA; [3]Planetary Science Institute, Tucson, AZ.

Introduction: Clay minerals found in stratigraphic sequences have been used to support the idea of widespread precipitation and pedogenic weathering during a warmer, wetter climate era on early Mars [e.g. 1-2]. These sequences have been identified in several provinces, including along the walls and on the plains surrounding Valles Marineris [3-5], in Mawrth Vallis [1,6], Meridiani [2,7-8], and Nili Fossae [9], and commonly exhibit Al-phyllosilicates overlying Mg/Fe-phyllosilicates.

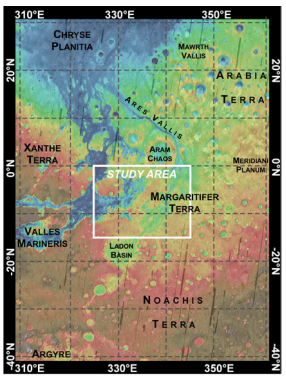

Fig. 1. *Regional context.*

The purpose of this study is to map and characterize surface to near-surface phyllosilicate-bearing deposits in West Margaritifer Terra, centrally located between the clay deposits around Valles Marineris and in Mawrth Vallis/Arabia Terra (Fig. 1). The geographic proximity to these other layered phyllosilicates suggests that a single regional formation mechanism is plausible, which would support the idea that a large, nearly contiguous area of the Noachian/Hesperian crust was subjected to an active and sustained hydrologic cycle [10]. However, West Margaritifer experienced significant fluvial erosion, catastrophic flooding, and chaos terrain development, providing other pathways for phyllosilicate formation, transport, and/or redeposition. Although adding geologic complexity, the presence of these landforms provides relative age and stratigraphic context that is key to deciphering the phyllosilicate formation timeline.

Datasets and Methodology: This study relies on multiple remote sensing datasets from several orbiting spacecraft. First, phyllosilicate outcrops were identified and delineated in an ArcGIS framework at ~1:250K scale using Compact Reconnaissance Imaging Spectrometer for Mars (CRISM) mapping data (180 m/pix). CRISM mapping data were processed to remove photometric and atmospheric effects as well as instrument residuals prior to the calculation of summary parameters (e.g., band depths) that were then mosiacked in 5°x5° tiles. All or part of 16 tiles cover the study area, which extends from 325°E to 345°E, 0°N to -15°N. All standard parameters [11] were examined, but D2300, which typically indicates the presence of Fe/Mg phyllosilicate, was the most commonly utilized. More than 130 high spatial and spectral resolution CRISM targeted observations (~20/40 m/pix) were also processed as Map-projected Targeted Reduced Data Records (MTRDRs) [12], comprising a suite of fully corrected spectral data, summary parameter cubes [11], and visual products that facilitate spectral analysis. Thermal Emission Imaging System (THEMIS) daytime IR controlled mosaics [13] and qualitative thermal inertia (TI) [14] at 100m/pix, Mars Orbiter Laser Altimeter (MOLA) 128 pix/deg gridded topography, and select High Resolution Stereo Camera (HRSC) DTMs served as basemaps. Tiled mosaics of Context Imager (CTX) data processed through the Projection on the Web (POW) utility [15] and High Resolution Imaging Science Experiment (HiRISE) data (including color and DTMs) were used to examine surface morphology.

Map units: We distinguish 4 phyllosilicate units with increasing levels of inference: certain, less certain, inferred–expanded, and inferred–buried (Figs. 2-3). *Certain* outcrops are observed directly in CRISM data and have strong spectral signatures. *Less certain* outcrops are also observed in CRISM data but are weaker or less spatially coherent. *Inferred–expanded* units encapsulate one or more surficial detections but are expanded based on the presence of coherent THEMIS TI and CTX data. Similarly, *inferred–buried* outcrops connect one or more impact-exhumed or fracture wall outcrops, suggest the widespread presence of the phyllosilicate layer in the shallow subsurface.

Regional Distribution: Phyllosilicate outcrops are distributed throughout the Noachian plateau region (Fig. 2), unconstrained by the youngest outflow channels, chasma, or chaos terrains and with no apparent elevation threshold. Outcrops exhibit higher thermal inertia than surroundings, signifying a relatively consolidated nature, and appear light-toned with polygonal fracturing in visible imagery. Three types of exposures all indicate shallow emplacement: a) surficial outcrops on plains, b) in fracture/chaos walls, and c) in crater rims and ejecta. Outcrops are consistently cross-cut by Hesperian-aged chaos and fractures.

Where exposed vertically, deposits can have variable thickness on the order of a few to several 10s of meters, sometimes with subparallel internal layering. Upper contacts tend to be relatively sharp, but determining the placement of the lower contact has proved elusive because of mass wasting. Superposed material, HiRISE color data suggests some vertical composition-

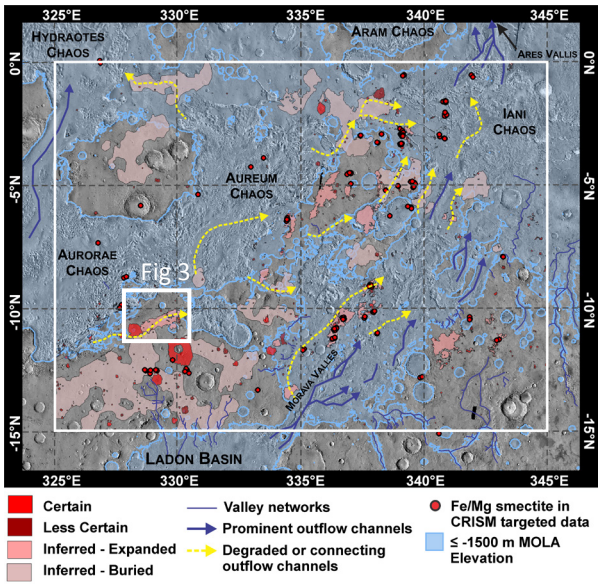

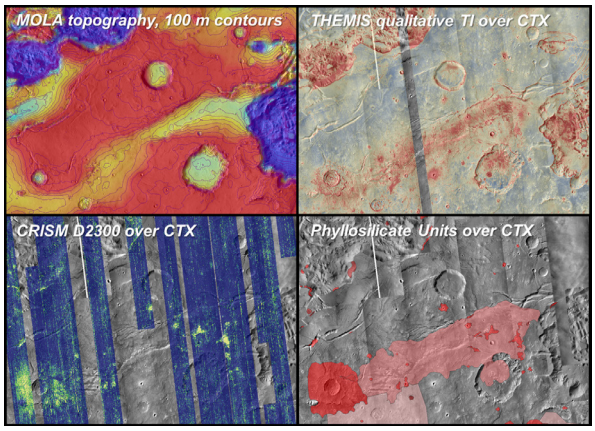

Fig. 2 (left). *Mapped units overlain on THEMIS day-IR with fluvial features highlighted. (Other identified minerals are not shown for simplicity.) Phyllosilicate outcrops occur both above and below the -1500 m elevation contour (blue shading), which correlate fairly well to the boundary of many basins, channel margins, and valley network terminations.*

Fig. 3 (right). *An example of an overland channel in topography and THEMIS TI (top), CRISM data phyllosilicate detections and defined units (lower) – see also Fig. 2.*

al variation with reddish light-toned material overlain by blueish material, but no spectral differences have been identified. Instead, hyperspectral data consistently show the phyllosilicate deposits to be dominated by Mg-smectite (e.g., saponite), which is similar to phyllosilicates identified to the west and southwest [3-5] and consistent with the recent findings of [16]. In contrast to some regional outcrops, however, no Al-phyllosilicates are observed to overly the Fe/Mg smectite. Other mineral species (zeolite, chloride) are observed in only a few instances. Low-calcium pyroxene is fairly common on the plateaus in small exposures, consistent with other Noachian-aged highland terrains.

Emplacement Mechanism(s): Our mapping results and observations can be compared to those expected from 4 formation mechanisms (fluviolacustrine, pedogenic, diagenetic, or hydrothermal) to determine the most likely scenario. The region-wide occurrence and spectral homogeneity of Mg-smectite disfavors emplacement by a hydrothermal process, where zonation or a regional gradient would be expected. The shallowness of the outcrops and lack of significant vertical variability similarly contradicts burial diagenesis, although deposition of a fine-grained air fall layer with subsequent alteration by ground water could be feasible. The paucity of Al-phyllosilicate does not necessarily rule out pedogenic weathering; however, it does suggest either an immature profile and/or mechanical stripping of the uppermost Al-bearing layer(s). Fluviolacustrine deposition likewise cannot fully explain the spatial distribution of outcrops, although the location of some prominent outcrops alongside channels or at basin margins may suggest at least some of the outcrops could have been emplaced in low energy aqueous environments [e.g., 17]. Given these observations, we favor the following formational sequence: 1) air fall deposition of ash or other fine-grained material, 2) fluvial or aeolian redistribution toward local topographic lows, 3a) regional pedogenic weathering or shallow groundwater diagenesis, 3b) burial by spectrally neutral dark-toned material or lava flows, 4) partial fluvial scouring and/or mobilization, 5) partial exposure via impact, chaos/fracture formation, or surface weathering.

Conclusion and Future Work: Mapping and characterization of phyllosilicate outcrops in West Margaritifer Terra reveals that a continuation of the regional layer observed to the west along Valles Marineris and NW Noachis Terra is feasible, but significant fluviolacustrine activity likely played an important role in redistributing and perhaps concentrating the clay-bearing material. Additional morphologic characterization using CTX and HiRISE DTMs will allow us to evaluate regional variation in layer thickness, dip, and internal structures to further constrain emplacement and implications for Mars' Noachian climate history.

References: [1] Noe Dobrea, E. Z., et al. (2010), *JGR, 115(E00D19)*. [2] Poulet, F., et al. (2005), *Nature, 438(7068)*. [3] Le Diet, L. et al. (2012), *JGR, 117(E00J05)*. [4] Buczkowski, D. L., et al. (2010), *41st LPSC*, Abstract #1458. [5] Loizeau et al. (2016) *47th LPSC*, Abstract #2280. [6] McKeown, N. K., et al. (2009), *JGR, 114(E00D10)*. [7] Wiseman, S. M., et al. (2010), *JGR, 115(E00D18)*. [8] Wiseman, S. M., et al. (2008), *GRL, 35(L19204)*. [9] Mustard, J. F. et al. (2009), *JGR, 114(E00D12)*. [10] Andrews-Hanna, J. C., and R. J. Phillips (2007), *JGR, 112(E08001)*. [11] Seelos, F. P. et al., (2014) *USGS Open File Report 2014-1056*. [12] Viviano-Beck, C. E., et al., (2014) *JGR, 119,* 1403–1431. [13] Fergason, R. L., et al. (2013), *44th LPSC*, Abstract #1642. [14] Fergason, R. L., et al. (2006), *JGR, 111(E12004)*. [15] Hare, T. M., et al. (2014), *45th LPSC*, Abstract #2487. [16] Thomas, R. et al. (2017) *JGR*, doi: 10.1002/2016FE005183. [17] Salvatore, M. R., et al. (2015) *JGR, 121* 273-295.